Published in final edited form as:

Abdom Radiol (NY). 2023 October ; 48(10): 3162–3173. doi:10.1007/s00261-023-04000-1.

Diagnosis of chronic pancreatitis using semi-quantitative MRI features of the pancreatic parenchyma: results from the multi-institutional MINIMAP study

Temel Tirkes[1,18], **Dhiraj Yadav**[2], **Darwin L. Conwell**[3], **Paul R. Territo**[4], **Xuandong Zhao**[1], **Scott A. Persohn**[5], **Anil K. Dasyam**[6], **Zarine K. Shah**[7], **Sudhakar K. Venkatesh**[8], **Naoki Takahashi**[8], **Ashley Wachsman**[9], **Liang Li**[10], **Yan Li**[10], **Stephen J. Pandol**[11], **Walter G. Park**[12], **Santhi Swaroop Vege**[13], **Phil A. Hart**[14], **Mark Topazian**[15], **Dana K. Andersen**[16], **Evan L. Fogel**[17] **Consortium for the Study of Chronic Pancreatitis, Diabetes, Pancreatic Cancer (CPDPC)**

[1] Department of Radiology and Imaging Sciences, Indiana University School of Medicine, Indianapolis, IN 46202, USA

[2] Division of Gastroenterology, Hepatology & Nutrition, Department of Medicine, University of Pittsburgh School of Medicine, Pittsburgh, PA, USA

[3] Department of Internal Medicine, University of Kentucky College of Medicine, Lexington, KY, USA

[4] Division of Clinical Pharmacology, Stark Neurosciences Research Institute, Radiology and Imaging Sciences, Indiana University School of Medicine, Indianapolis, IN 46202, USA

[5] Stark Neurosciences Research Institute, Indiana University School of Medicine, Indianapolis, IN 46202, USA

[6] Department of Radiology, University of Pittsburgh Medical Center, Pittsburgh, PA, USA

[7] Department of Radiology, The Ohio State University Wexner Medical Center, Columbus, OH, USA

[8] Department of Radiology, Mayo Clinic, Rochester, MN, USA

[9] Department of Imaging, University of California in Los Angeles, Los Angeles, CA, USA

[10] Department of Biostatistics, The University of Texas MD Anderson Cancer Center, Houston, TX, USA

[11] Division of Digestive and Liver Diseases, Cedars-Sinai Medical Center, Los Angeles, CA, USA

✉ Temel Tirkes atirkes@iu.edu.

Conflict of interest The authors declare that they have no conflict of interest.

Supplementary Information The online version contains supplementary material available at https://doi.org/10.1007/s00261-023-04000-1.

[12] Division of Gastroenterology and Hepatology, Department of Medicine, Stanford University Medical Center, Stanford, CA, USA

[13] Department of Internal Medicine, Mayo Clinic, Rochester, MN, USA

[14] Division of Gastroenterology, Hepatology & Nutrition, The Ohio State University Wexner Medical Center, Columbus, OH, USA

[15] Mayo Clinic, Rochester, MN, USA

[16] Division of Digestive Diseases and Nutrition, National Institute of Diabetes and Digestive and Kidney Diseases, National Institutes of Health, Bethesda, MD, USA

[17] Lehman, Bucksot and Sherman Section of Pancreatobiliary Endoscopy, Indiana University School of Medicine, Indianapolis, IN, USA

[18] Department of Radiology and Imaging Sciences, Indiana University School of Medicine, 550 N. University Blvd. Suite 0663, Indianapolis, IN 46202, USA

Abstract

Purpose—To determine the diagnostic performance of parenchymal MRI features differentiating CP from controls.

Methods—This prospective study performed abdominal MRI scans at seven institutions, using 1.5 T Siemens and GE scanners, in 50 control and 51 definite CP participants, from February 2019 to May 2021. MRI parameters included the T1-weighted signal intensity ratio of the pancreas (T1 score), arterial-to-venous enhancement ratio (AVR) during venous and delayed phases, pancreas volume, and diameter. We evaluated the diagnostic performance of these parameters individually and two semi-quantitative MRI scores derived using logistic regression: SQ-MRI Model A (T1 score, AVR venous, and tail diameter) and Model B (T1 score, AVR venous, and volume).

Results—When compared to controls, CP participants showed a significantly lower mean T1 score (1.11 vs. 1.29), AVR venous (0.86 vs. 1.45), AVR delayed (1.07 vs. 1.57), volume (54.97 vs. 80.00 ml), and diameter of the head (2.05 vs. 2.39 cm), body (2.25 vs. 2.58 cm), and tail (1.98 vs. 2.51 cm) ($p < 0.05$ for all). AUCs for these individual MR parameters ranged from 0.66 to 0.79, while AUCs for the SQ-MRI scores were 0.82 and 0.81 for Model A (T1 score, AVR venous, and tail diameter) and Model B (T1 score, AVR venous, and volume), respectively. After propensity-matching adjustments for covariates, AUCs for Models A and B of the SQ-MRI scores increased to 0.92 and 0.93, respectively.

Conclusion—Semi-quantitative parameters of the pancreatic parenchyma, including T1 score, enhancement ratio, pancreas volume, diameter and multi-parametric models combining these parameters are helpful in diagnosis of CP. Longitudinal analyses including more extensive population are warranted to develop new diagnostic criteria for CP.

Graphical Abstract

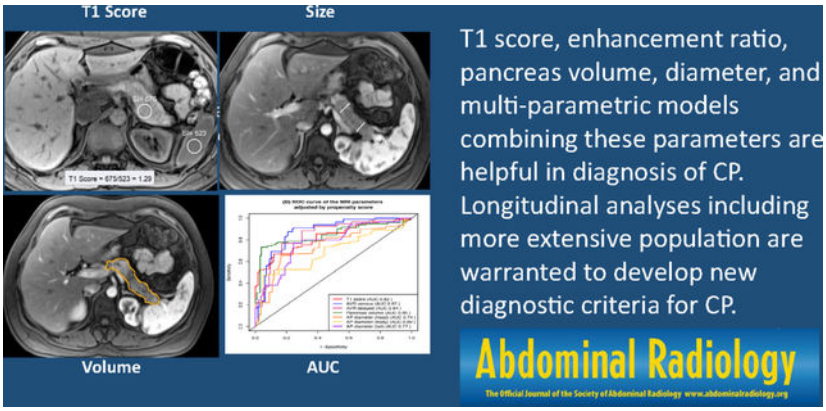

Keywords

Chronic pancreatitis; T1; MRI; Volume; Size; Enhancement

Introduction

Chronic pancreatitis (CP) is a multifactorial, fibroinflammatory syndrome resulting in chronic pain, exocrine and endocrine pancreatic insufficiency, reduced quality of life, and a shorter life expectancy [1]. The incidence and prevalence of chronic pancreatitis are rising, and no curative treatment is available yet [1]. Computerized tomography (CT) and magnetic resonance imaging (MRI) with magnetic resonance cholangiopancreatography (MRCP) are recommended as the first-line diagnostic modalities for CP [2]. The Cambridge classification was developed for endoscopic retrograde cholangiopancreatography (ERCP) in the 1980s [3] and has been adopted for MRCP [4]. This classification primarily captures evidence of periductal fibrosis and does not reflect the parenchymal fibrosis or loss of acinar tissue (included in the histopathologic triad for diagnosis of CP) [5]. This is a critical limitation since the ductal system comprises only 4% of the pancreas whereas acinar cells are over 80% [6–8]. Besides, age-related increases in pancreatic duct diameter have been reported in subjects without CP [9]. Furthermore, there is variability in the interpretation of ductal changes [10], measurements [11] and moderate interobserver agreement for assessing Cambridge grade [12, 13]. Due to these limitations, the diagnosis of CP can be elusive or delayed [14, 15]. Potential for pancreatic parenchymal features (such as T1 signal intensity ratio (SIR) using T1-weighted images, T1 relaxation time using MR relaxometry, pancreas volume, pancreatic steatosis, and extracellular volume fraction) to provide superior diagnostic value has been previously suggested by retrospective studies, expert panel reviews and mentioned in consensus statements [16–18]. However, these parameters have yet to be evaluated in a prospective, multi-institutional setting to be incorporated into the diagnostic criteria. We present the results of the Magnetic Resonance Imaging as a Non-Invasive Method for the Assessment of Pancreatic Fibrosis (MINIMAP) study [19], which is an ancillary study within the Consortium for the Study of Chronic Pancreatitis, Diabetes, and Pancreatic Cancer (CPDPC) [20]. The MINIMAP is the first prospective, multi-institutional study exploring the potential of parenchymal MRI features as an imaging biomarker for CP [19].

Materials and methods

Study population

We invited eligible participants who enrolled in the CPDPC longitudinal cohort study, Prospective Evaluation of Chronic Pancreatitis for Epidemiologic and Translational Studies (PROCEED) (NCT03099850) [21] at seven enrolling centers to undergo a research MRI for the MINIMAP study. Enrolling centers were Indiana University in Indianapolis, IN; the University of Pittsburgh Medical Center in Pittsburgh, PA; The Ohio State University Wexner Medical Center in Columbus, OH; Mayo Clinic in Rochester, MN; Stanford University in Stanford, CA; Cedars-Sinai Medical Center in Los Angeles, CA; The University of California Los Angeles Medical Center in Los Angeles, CA and data coordinating center was at The University of Texas MD Anderson Cancer Center in Houston, TX. Institutional review board approval was obtained at each center, and all participants signed a written informed consent form prior to the study procedures. The MINIMAP study protocol has been published and describes the enrollment algorithm with a flow diagram, inclusion/exclusion criteria, sample size calculation, and data collection points [19]. One hundred thirty-seven controls and CP participants agreed and signed consent forms between February 2019 and May 2021, and 123 completed the imaging. After excluding 22 MRIs for the reasons listed in Fig. 1, 101 MRI examinations were available for image analysis. There were 50 controls (no pancreas disease, no abdominal symptoms, and no personal or family history of pancreatic disease) and 51 participants with confirmed CP (history of recurrent pancreatitis with Cambridge grade 3 or 4 by MRCP or presence of calcifications on CT scan) [21]. The MINIMAP study published the results of quantitative MRI features in a separate paper [22].

MR imaging

All MRI examinations were performed on 1.5 T Siemens (Siemens Healthcare, Malvern, PA) or GE (GE Healthcare, Chicago, IL) scanners. The MRI protocol can be found in Table S1 of the supplemental materials section [19].

Image analysis

Image data collection was performed by a former MRI technologist, a professional image analysis scientist (SAP) with 18 years of experience. He was blinded to any clinical information or cohort assignment and data collection was supervised by radiologist (TT). After the images were imported into MIM (v7.05, MIM Software, Beachwood, OH), different sequences were co-registered via manual registration and exported as DICOM files. The region of interest (ROI) size was at least 1 c m^2 and enlarged by the size of the anatomical region of the pancreatic head, body, and tail. A simple average was used for the analysis. Unenhanced T1-weighted (T1W) signal intensities were measured by placing an ROI in a homogenous area of the pancreas. The spleen was used as a reference organ to calculate the T1 SIR (or T1 score) (Fig. 2A and B) using the formula:

$$\text{T1 SIR (score)} = \frac{\text{T1W signal pancreas unenhanced}}{\text{T1W signal spleen unenhanced}}$$

Arterial-to-venous enhancement ratio (AVR) was calculated by measuring the T1W signal during the unenhanced, arterial, venous, and 5-min delayed phases using the formula:

$$\text{AVR} = \frac{\text{T1W signal arterial-T1W signal unenhanced}}{\text{T1W signal venous or delayed-T1W signal unenhanced}}$$

The diameter of the pancreas was measured in the thickest portion of the head, body, and tail of the pancreas with a caliper tool placed perpendicular to the main pancreatic duct (axis of the pancreas) [23] (Fig. 2C and D). The largest diameter of the pancreas located to the right side of the superior mesenteric artery was considered the head. The body of the pancreas was measured anterior to the left lateral margin of the vertebral body, and the tail was measured distal to the left lateral margin of the left kidney. The pancreas volume was measured using MIM software by manual segmentation on arterial phase T1-weighted post-contrast series. Each voxel's x, y, and z dimensions were multiplied by the number of voxels in the region of interest to compute the final volume (Fig. 2E).

Statistical analysis

We used two-sample t-tests to compare the mean values of individual MRI parameters between the controls and CP participants. We used receiver operating characteristics (ROC) curve analysis to assess the performance of each MRI parameter for the diagnosis of CP.

We fitted a logistic regression with disease status (CP vs. control) as the dependent variable and various MRI parameters as independent variables. The linear predictor of this logistic model is the optimal composite score since combining multiple parameters maximizes the area under the ROC curve (AUC) as long as the logistic regression model is correctly specified [24]. We derived two semi-quantitative MRI (SQ-MRI) scores based on different logistic regression models. Model A included the T1 score, AVR venous, and the diameter in the tail, while Model B included the T1 score, AVR venous, and the pancreas volume. These two models were selected from pre-specified candidate models with various MRI parameters. The results of all candidate models can be found in Table S2 of the supplemental section. Based on the fitted regression coefficients, the two SQ – MRI scores were computed as follows:

$$\begin{aligned}\text{SQ-MRI scone A} = 7.7395 &- (2.2772 \times \text{T1 scone}) \\ &- (1.9308 \times \text{ AVR venous}) \\ &- (1.2621 \times \text{ tail diameter})\end{aligned}$$

$$\begin{aligned}\text{SQ} - \text{MRI scone B} = 5.9813 &- (2.1114 \times \text{T1 score}) \\ &- (1.7270 \times \text{ AVR venous}) \\ &- (0.0219 \times \text{ pancreas volume})\end{aligned}$$

Unlike the ROC analysis on individual MRI parameters, we used cross-validation when calculating the AUC of SQ-MRI since SQ-MRI was derived from an estimated statistical model and was necessary to protect against overfitting. Specifically, a bootstrap sample taken from the original dataset was used to estimate the logistic model. The AUC was calculated by applying that model to participants not selected for the bootstrap dataset. This

process was repeated 200 times randomly, and the average AUC was the cross-validated AUC for the SQ-MRI score.

Demographics and behavioral covariates may confound the association between MRI parameters and disease status (CP or control). To reduce the confounding effect, we used propensity score weighting to balance the distribution (Table 1) between CP and controls, followed by a ROC analysis on propensity score weighted data [25]. The propensity scores were estimated by the covariate balancing propensity score (CBPS) algorithm [26] with inverse probability weighting. We also used linear models to study the association between each MRI parameter and pre-specified demographics, behavioral, and clinical covariates. This analysis was limited to CP participants as the covariates included variables-related explicitly to CP.

Results

Demographic, behavioral risk factors and clinical findings of the study population are listed in Table 1.

MRI parameters in controls vs. CP

The boxplot distribution of the seven MRI parameters is shown in Fig. 3A–G. The test statistics, their significance levels, and the summary statistics of these parameters in the two groups are reported in Table 2. Compared with the controls, CP participants had a significantly lower mean T1 score, AVR venous, AVR delayed, volume, and diameter in the head, body, and tail. Enhancement in the arterial phase was higher in the control group than in the CP participants ($p = 0.0003$). The mean enhancement in the venous and delayed phases was not significantly different between the two groups ($p = 0.07$ and $p = 0.06$, respectively). Figure 4A compares the ROC curves of the various MRI parameters and their corresponding AUCs. Table S3 in the supplemental materials shows the sensitivity and specificity for selected thresholds of the MRI parameters.

SQ-MRI scores

Table 2, Fig. 3H, and I compare the SQ-MRI scores (Models A and B) between the control and CP groups. The estimated AUC from internal cross-validation was 0.82 for Model A and 0.81 for Model B (Table 2), which are less than without cross-validation but higher than the individual MRI parameters that compose the SQ-MRI scores.

Propensity score-adjusted ROC analysis

Figure 4B compares the weighted ROC curves for seven MRI parameters. Propensity score-adjusted AUCs for T1 score, AVR venous, AVR delayed, pancreas volume, and head, body, and tail diameters were 0.82, 0.87, 0.84, 0.85, 0.74, 0.69, and 0.77, respectively. The propensity score-adjusted AUCs for SQ-MRI scores showed the highest diagnostic performance: 0.92 for Model A and 0.93 for Model B.

Impact of demographic and disease-related risk factors on MRI parameters in CP

Table 3 shows that T1 score, AVR venous, AVR delayed, pancreas volume, and head diameter did not correlate with any of the covariates ($p > 0.05$). There were sporadic statistically significant associations, suggesting that these MRI parameters quantify independent aspects of physiological conditions that are not explained by other patient characteristics.

Discussion

This is the first prospective study aimed to evaluate whether parenchymal MRI features can differentiate CP participants from controls. We assessed the T1W SIR (or T1 score), AVR in venous and delayed phases, volume, and diameter in the head, body, and tail of the pancreas. We evaluated the diagnostic performance of these parameters individually and also by two semi-quantitative MRI scores derived using logistic regression: SQ-MRI Model A (T1 score, AVR venous, and tail diameter) and SQ-MRI Model B (T1 score, AVR venous, and volume). We found that each parameter was significantly lower in the CP group. Both composite scores achieved better diagnostic performance compared to individual parameters, with an AUC value of 0.82 or 0.81. Propensity score-adjusted AUCs for SQ-MRI scores showed superior diagnostic performance: 0.92 for Model A and 0.93 for Model B. This study performed imaging at multiple centers using different MRI vendors; therefore, there is a high likelihood that our results will be reproducible compared to previous studies.

The pancreas is a highly productive exocrine gland of the digestive system secreting more than 1–2 liters of proteinaceous fluid per day containing digestive enzymes and bicarbonate [27, 28]. Attributed to the abundance of proteinaceous material in the acinar cells, the normal pancreas exhibits a relatively higher T1W signal intensity than other solid organs in the abdomen, as seen in Fig. 2A [29, 30]. The loss of T1W signal in our CP participants (average 1.11) vs. controls (average 1.29), as seen in Fig. 2B, corresponds to the loss of acinar cells replaced by fibrosis. This association is supported by studies that included surgical histopathology [29, 31–33] and reported a correlation of parenchymal MRI features (T1 SIR, T1 relaxation time, diffusion-weighted imaging, enhancement ratio, and MR elastography) with the degree of fibrosis. In addition to fibrosis, some studies have reported lower T1W signals in patients with exocrine pancreatic dysfunction (EPD) [14, 15, 34]. In one of these studies, including 60 surgical specimens, the T1 score and AVR had a higher correlation for pancreatic fibrosis than the Cambridge score [33]. If the spleen is removed or deemed unreliable (e.g., iron deposition), the T1 score can be obtained using the paraspinal muscle as a reference organ [35].

Diminished pancreatic size is a common, albeit non-specific feature of CP [5, 9]. Our study shows that the mean pancreas volume in CP participants was lower, 54.97 ml, compared to 80.0 ml in controls. A study by Szczepaniak et al. using MRI to evaluate the normal pancreas reported that the mean in vivo volume was 72.7 ml [36]. Schrader et al. used CT and reported the mean pancreas volumes to be 64.9 ml in CP patients and 82.3 ml in controls [37]. Faghih et al. used CT to assess pancreas volume in patients undergoing total pancreatectomy with islet cell autotransplantation [38]. The mean pancreatic volume for patients with RAP, indeterminate CP, and definite CP were 65.7 ml, 61.8 ml, and 54.9

ml, respectively. DeSouza et al. demonstrated a progressive loss of pancreas volume in 123 patients with RAP. The pancreas volume using MRI was significantly reduced in those with ≥ 3 AP episodes (70.2 ml) but not in those with one (85.8 ml) or two episodes (80.7 ml) compared with the healthy control group (87.7 ml) [39]. A more recent MRI study [9] measured pancreatic diameter in participants with no pancreas disease and reported a near-perfect inter-correlation coefficient (over 0.95) between the two readers. In addition to CP, an age-related decrease in pancreatic size has also been reported [9, 23, 40].

Our results showed that the arterial phase enhancement of the pancreas was lower in CP participants. However, enhancement in the venous and delayed phases was not significantly different between the two groups. The impaired hemodynamics of the pancreas has been shown in animal models with acute and chronic pancreatitis [41, 42]. A limited number of human studies have evaluated the enhancement characteristics in CP. One study compared AVR in 36 patients with suspected CP undergoing ePFT and reported no difference between the normal and abnormal ePFT groups [34]. The second study included 26 subjects with suspected CP and reported the correlation ($r = 0.466$) between the AVR and the degree of duodenal filling after secretin administration [15].

The statistically small sample size was the main limitation of this pilot study. Based on results of this study, more extensive studies are needed including RAP participants and longitudinal analyses. Due to the small sample size, the weighted AUCs for the SQ-MRI scores were not calculated with internal cross-validation and might be slightly overfitted. However, the effect of overfitting is expected to be very mild, since the observed overfitting from the AUC of the SQ-MRI scores in the analysis above, without propensity score adjustment is small (Model A: 0.82 vs. 0.85 with/without cross-validation; Model B: 0.81 vs. 0.84 with/without cross-validation). Image non-uniformity in MRI can be a problem, primarily due to B1 field inhomogeneity, which results in inconsistent flip angles across the image planes [43]. Hardware vendors provide standard methods to minimize inhomogeneity, such as the B1 normalization filter and phase array uniformity correction filter (e.g., pre-scan normalization) [43, 44]. Our study used B1 maps to improve potential problem of image homogeneity.

Our results verify the benefit of parenchymal MR imaging in diagnosing CP and underscore the necessity for a new comprehensive diagnostic criteria to include parenchymal and ductal features. Semi-quantitative parameters of the pancreatic parenchyma (T1 score, enhancement ratio, volume, and diameter) are significantly lower in CP compared to controls. Longitudinal analyses including more extensive population are warranted to develop new diagnostic criteria for CP.

Conclusion

This prospective, multi-institutional, multi-vendor study verifies that parenchymal MRI features, including T1 score, arterial-to-venous enhancement ratio, pancreas volume, diameter and multi-parametric logistic regression models combining these parameters provide high diagnostic performance for CP. Future studies are warranted using more extensive study populations and longitudinal analyses. We should be able to develop a

more comprehensive imaging biomarker combining the parenchymal and ductal features. Such a biomarker for CP would allow population-based comparisons and cross-platform compatibility when used in clinical practice or clinical trials.

Supplementary Material

Refer to Web version on PubMed Central for supplementary material.

Funding

Research reported in this publication was supported by National Cancer Institute and National Institute of Diabetes and Digestive and Kidney Diseases of the National Institutes of Health under award numbers related to: the MINIMAP study (R01DK116963) and The Consortium for the Study of Chronic Pancreatitis, Diabetes, and Pancreatic Cancer (CPDPC) under award numbers: U01DK108328 (CDMC), U01DK108323 (IU), U01DK108306 (UPMC), U01DK108327 (OSU), U01DK108327 (CSMC), DKP3041301 (UCLA), U01DK108300 (Stanford) and U01DK108288 (Mayo Clinic). The content is solely the responsibility of the authors and does not necessarily represent the official views of the National Institutes of Health.

Abbreviations

CP	Chronic pancreatitis
RAP	Recurrent acute pancreatitis
MRI	Magnetic resonance imaging
SQ-MRI	Semi-quantitative MRI
AVR	Arterial-to-venous enhancement ratio
EPD	Exocrine pancreatic dysfunction
ePFT	Endoscopic pancreatic function test
MRCP	Magnetic resonance cholangiopancreatography
CPDPC	Consortium for the Study of Chronic Pancreatitis, Diabetes, and Pancreatic Cancer
MINIMAP	Magnetic resonance imaging as a non-invasive method for the assessment of pancreatic fibrosis
PROCEED	Prospective evaluation of chronic pancreatitis for epidemiologic and translational studies

References

1. Beyer G, Habtezion A, Werner J, Lerch MM, Mayerle J. Chronic pancreatitis. Lancet. 2020;396(10249):499–512. 10.1016/S0140-6736(20)31318-0. [PubMed: 32798493]
2. Gardner TB, Adler DG, Forsmark CE, Sauer BG, Taylor JR, Whitcomb DC. ACG Clinical Guideline: Chronic Pancreatitis. Am J Gastroenterol. 2020;115(3):322–39. 10.14309/ajg.0000000000000535. [PubMed: 32022720]
3. Sarner M, Cotton PB. Classification of pancreatitis. Gut. 1984;25(7):756–9. 10.1136/gut.25.7.756. [PubMed: 6735257]

4. Conwell DL, Lee LS, Yadav D, Longnecker DS, Miller FH, Mortele KJ, et al. American Pancreatic Association Practice Guidelines in Chronic Pancreatitis: evidence-based report on diagnostic guidelines. Pancreas. 2014;43(8):1143–62. 10.1097/MPA.0000000000000237. [PubMed: 25333398]
5. Esposito I, Hruban RH, Verbeke C, Terris B, Zamboni G, Scarpa A, et al. Guidelines on the histopathology of chronic pancreatitis. Recommendations from the working group for the international consensus guidelines for chronic pancreatitis in collaboration with the International Association of Pancreatology, the American Pancreatic Association, the Japan Pancreas Society, and the European Pancreatic Club. Pancreatology. 2020;20(4):586–93. 10.1016/j.pan.2020.04.009. [PubMed: 32414657]
6. Atkinson MA, Campbell-Thompson M, Kusmartseva I, Kaestner KH. Organisation of the human pancreas in health and in diabetes. Diabetologia. 2020;63(10):1966–73. 10.1007/s00125-020-05203-7. [PubMed: 32894306]
7. Barreto SG, Carati CJ, Toouli J, Saccone GT. The islet-acinar axis of the pancreas: more than just insulin. Am J Physiol Gastrointest Liver Physiol. 2010;299(1):G10–22. 10.1152/ajpgi.00077.2010. [PubMed: 20395539]
8. Tang X, Kusmartseva I, Kulkarni S, Posgai A, Speier S, Schatz DA, et al. Image-Based Machine Learning Algorithms for Disease Characterization in the Human Type 1 Diabetes Pancreas. Am J Pathol. 2021;191(3):454–62. 10.1016/j.ajpath.2020.11.010. [PubMed: 33307036]
9. Wang Q, Swensson J, Hu M, Cui E, Tirkes T, Jennings SG, et al. Distribution and correlation of pancreatic gland size and duct diameters on MRCP in patients without evidence of pancreatic disease. Abdom Radiol (NY). 2019;44(3):967–75. 10.1007/s00261-018-1879-3. [PubMed: 30600375]
10. Swensson J, Akisik F, Collins D, Olesen SS, Drewes AM, Frokjaer JB. Is Cambridge scoring in chronic pancreatitis the same using ERCP and MRCP?: A need for revision of standards. Abdom Radiol (NY). 2021;46(2):647–54. 10.1007/s00261-020-02685-2. [PubMed: 32740862]
11. Borgbjerg J, Steinkohl E, Olesen SS, Akisik F, Bethke A, Bieliuniene E, et al. Inter- and intra-observer variability of computed tomography-based parenchymal- and ductal diameters in chronic pancreatitis: a multi-observer international study. Abdom Radiol (NY). 2023;48(1):306–17. 10.1007/s00261-022-03667-2. [PubMed: 36138242]
12. Tirkes T, Shah ZK, Takahashi N, Grajo JR, Chang ST, Wachsman AM, et al. Inter-observer variability of radiologists for Cambridge classification of chronic pancreatitis using CT and MRCP: results from a large multi-center study. Abdom Radiol (NY). 2020;45(5):1481–7. 10.1007/s00261-020-02521-7. [PubMed: 32285180]
13. Trout AT, Abu-El-Haija M, Anupindi SA, Marine MB, Murati M, Phelps AS, et al. Interobserver Agreement for CT and MRI Findings of Chronic Pancreatitis in Children: A Multicenter Ancillary Study Under the INSPPIRE Consortium. American Journal of Roentgenology. 2022. 10.2214/AJR.21.27234.
14. Tirkes T, Fogel EL, Sherman S, Lin C, Swensson J, Akisik F, et al. Detection of exocrine dysfunction by MRI in patients with early chronic pancreatitis. Abdom Radiol (NY). 2017;42(2):544–51. 10.1007/s00261-016-0917-2. [PubMed: 27660281]
15. Balci NC, Alkaade S, Magas L, Momtahen AJ, Burton FR. Suspected chronic pancreatitis with normal MRCP: findings on MRI in correlation with secretin MRCP. J Magn Reson Imaging. 2008;27(1):125–31. 10.1002/jmri.21241. [PubMed: 18058927]
16. Frokjaer JB, Akisik F, Farooq A, Akpinar B, Dasyam A, Drewes AM, et al. Guidelines for the Diagnostic Cross Sectional Imaging and Severity Scoring of Chronic Pancreatitis. Pancreatology. 2018;18(7):764–73. 10.1016/j.pan.2018.08.012. [PubMed: 30177434]
17. Tirkes T, Shah ZK, Takahashi N, Grajo JR, Chang ST, Venkatesh SK, et al. Reporting Standards for Chronic Pancreatitis by Using CT, MRI, and MR Cholangiopancreatography: The Consortium for the Study of Chronic Pancreatitis, Diabetes, and Pancreatic Cancer. Radiology. 2019;290(1):207–15. 10.1148/radiol.2018181353. [PubMed: 30325281]
18. Steinkohl E, Olesen SS, Mark EB, Hansen TM, Frandsen LK, Drewes AM, et al. Progression of parenchymal and ductal findings in patients with chronic pancreatitis: A 4-year follow-up MRI study. Eur J Radiol. 2020;125:108868. 10.1016/j.ejrad.2020.108868. [PubMed: 32070871]

19. Tirkes T, Yadav D, Conwell DL, Territo PR, Zhao X, Venkatesh SK, et al. Magnetic resonance imaging as a non-invasive method for the assessment of pancreatic fibrosis (MINIMAP): a comprehensive study design from the consortium for the study of chronic pancreatitis, diabetes, and pancreatic cancer. Abdom Radiol (NY). 2019;44(8):2809–21. 10.1007/s00261-019-2049-5. [PubMed: 31089778]
20. Serrano J, Andersen DK, Forsmark CE, Pandol SJ, Feng Z, Srivastava S, et al. Consortium for the Study of Chronic Pancreatitis, Diabetes, and Pancreatic Cancer: From Concept to Reality. Pancreas. 2018;47(10):1208–12. 10.1097/MPA.0000000000001167. [PubMed: 30325859]
21. Yadav D, Park WG, Fogel EL, Li L, Chari ST, Feng Z, et al. PROspective Evaluation of Chronic Pancreatitis for EpidEmiologic and Translational StuDies: Rationale and Study Design for PROCEED From the Consortium for the Study of Chronic Pancreatitis, Diabetes, and Pancreatic Cancer. Pancreas. 2018;47(10):1229–38. 10.1097/MPA.0000000000001170. [PubMed: 30325862]
22. Tirkes T, Yadav D, Conwell DL, Territo PR, Zhao X, Persohn SA, et al. Quantitative MRI of chronic pancreatitis: results from a multi-institutional prospective study, magnetic resonance imaging as a non-invasive method for assessment of pancreatic fibrosis (MINIMAP). Abdom Radiol (NY). 2022;47(11):3792–805. 10.1007/261-022-03654-7. [PubMed: 36038644]
23. Heuck A, Maubach PA, Reiser M, Feuerbach S, Allgayer B, Lukas P, et al. Age-related morphology of the normal pancreas on computed tomography. Gastrointest Radiol. 1987;12(1):18–22. 10.1007/BF01885094. [PubMed: 3792751]
24. Pepe MS, Etzioni R, Feng Z, Potter JD, Thompson ML, Thornquist M, et al. Phases of biomarker development for early detection of cancer. J Natl Cancer Inst. 2001;93(14):1054–61. 10.1093/jnci/93.14.1054. [PubMed: 11459866]
25. Le Borgne F, Combescure C, Gillaizeau F, Giral M, Chapal M, Giraudeau B, et al. Standardized and weighted time-dependent receiver operating characteristic curves to evaluate the intrinsic prognostic capacities of a marker by taking into account confounding factors. Stat Methods Med Res. 2018;27(11):3397–410. 10.1177/0962280217702416. [PubMed: 28633603]
26. Imai K, Ratkovic M. Covariate Balancing Propensity Score. Journal of the Royal Statistical Society: Series B. 2014;76(1):243–63.
27. Ishiguro H, Yamamoto A, Nakakuki M, Yi L, Ishiguro M, Yamaguchi M, et al. Physiology and pathophysiology of bicarbonate secretion by pancreatic duct epithelium. Nagoya J Med Sci. 2012;74(1–2):1–18. [PubMed: 22515107]
28. Pandol SJ. Water and Ion Secretion from the Pancreatic Ductal System. The Exocrine Pancreas. Morgan & Claypool Life Sciences; 2010.
29. Watanabe H, Kanematsu M, Tanaka K, Osada S, Tomita H, Hara A, et al. Fibrosis and postoperative fistula of the pancreas: correlation with MR imaging findings--preliminary results. Radiology. 2014;270(3):791–9. 10.1148/radiol.13131194. [PubMed: 24475834]
30. Winston CB, Mitchell DG, Outwater EK, Ehrlich SM. Pancreatic signal intensity on T1-weighted fat saturation MR images: clinical correlation. J Magn Reson Imaging. 1995;5(3):267–71. 10.1002/jmri.1880050307. [PubMed: 7633102]
31. Trikudanathan G, Walker SP, Munigala S, Spilseth B, Malli A, Han Y, et al. Diagnostic Performance of Contrast-Enhanced MRI With Secretin-Stimulated MRCP for Non-Calcific Chronic Pancreatitis: A Comparison With Histopathology. Am J Gastroenterol. 2015;110(11):1598–606. 10.1038/ajg.2015.297. [PubMed: 26372506]
32. Liu C, Shi Y, Lan G, Xu Y, Yang F. Evaluation of Pancreatic Fibrosis Grading by Multiparametric Quantitative Magnetic Resonance Imaging. J Magn Reson Imaging. 2021;54(5):1417–29. 10.1002/jmri.27626. [PubMed: 33819364]
33. Tirkes T, Saeed OA, Osuji VC, Kranz CE, Roth AA, Patel AA, et al. Histopathologic correlation of pancreatic fibrosis with pancreatic magnetic resonance imaging quantitative metrics and Cambridge classification. Abdom Radiol (NY). 2022. 10.1007/s00261-022-03532-2.
34. Balci NC, Smith A, Momtahen AJ, Alkaade S, Fattahi R, Tariq S, et al. MRI and S-MRCP findings in patients with suspected chronic pancreatitis: correlation with endoscopic pancreatic function testing (ePFT). J Magn Reson Imaging. 2010;31(3):601–6. 10.1002/jmri.22085. [PubMed: 20187202]

35. Tirkes T, Dasyam AK, Shah ZK, Fogel EL, Vege SS, Li L, et al. T1 signal intensity ratio of the pancreas as an imaging biomarker for the staging of chronic pancreatitis. Abdom Radiol (NY). 2022;47(10):3507–19. 10.1007/s00261-022-03611-4. [PubMed: 35857066]

36. Szczepaniak EW, Malliaras K, Nelson MD, Szczepaniak LS. Measurement of pancreatic volume by abdominal MRI: a validation study. PLoS One. 2013;8(2):e55991. 10.1371/journal.pone.0055991. [PubMed: 23418491]

37. Schrader H, Menge BA, Schneider S, Belyaev O, Tannapfel A, Uhl W, et al. Reduced pancreatic volume and beta-cell area in patients with chronic pancreatitis. Gastroenterology. 2009;136(2):513–22. 10.1053/j.gastro.2008.10.083. [PubMed: 19041312]

38. Faghih M, Noe M, Mannan R, Kamel IR, Zaheer A, Kalyani RR, et al. Pancreatic volume does not correlate with histologic fibrosis in adult patients with recurrent acute and chronic pancreatitis. Pancreatology. 2020;20(6):1078–84. 10.1016/j.pan.2020.07.409. [PubMed: 32819846]

39. DeSouza SV, Priya S, Cho J, Singh RG, Petrov MS. Pancreas shrinkage following recurrent acute pancreatitis: an MRI study. Eur Radiol. 2019;29(7):3746–56. 10.1007/s00330-019-06126-7. [PubMed: 30980124]

40. Rajan E, Clain JE, Levy MJ, Norton ID, Wang KK, Wiersema MJ, et al. Age-related changes in the pancreas identified by EUS: a prospective evaluation. Gastrointest Endosc. 2005;61(3):401–6. 10.1016/s0016-5107(04)02758-0. [PubMed: 15758911]

41. Inoue K, Kawano T, Shima K, Suzuki TK, Tobe T, Yajima H. Relationship between development of fibrosis and hemodynamic changes of the pancreas in dogs. Gastroenterology. 1981;81(1):37–47. [PubMed: 7239124]

42. Reber HA, Karanjia ND, Alvarez C, Widdison AL, Leung FW, Ashley SW, et al. Pancreatic blood flow in cats with chronic pancreatitis. Gastroenterology. 1992;103(2):652–9. [PubMed: 1634080]

43. Felemban D, Verdonschot RG, Iwamoto Y, Uchiyama Y, Kakimoto N, Kreiborg S, et al. A quantitative experimental phantom study on MRI image uniformity. Dentomaxillofac Radiol. 2018;47(6):20180077. 10.1259/dmfr.20180077. [PubMed: 29718695]

44. Mihara H, Iriguchi N, Ueno S. A method of RF inhomogeneity correction in MR imaging. MAGMA. 1998;7(2):115–20. 10.1007/BF02592235. [PubMed: 9951771]

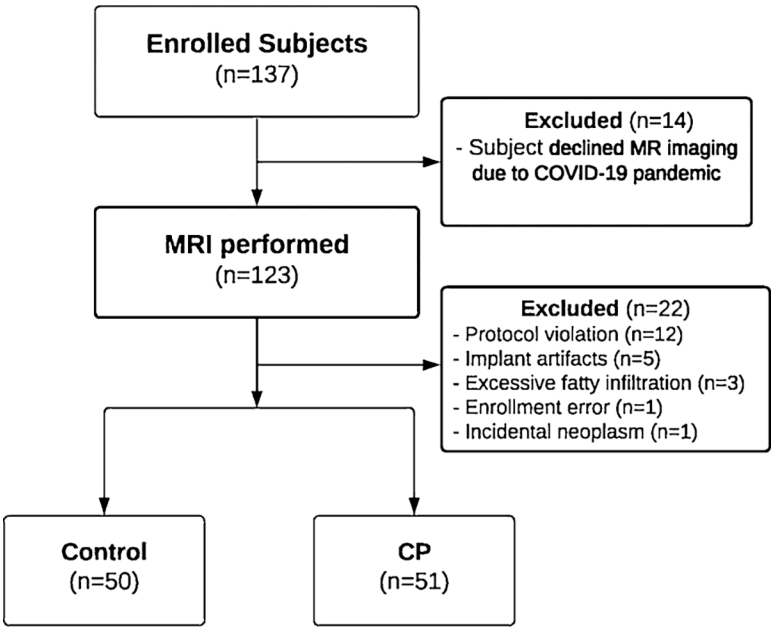

Fig. 1.
Flowchart of participant enrollment in the MINIMAP study

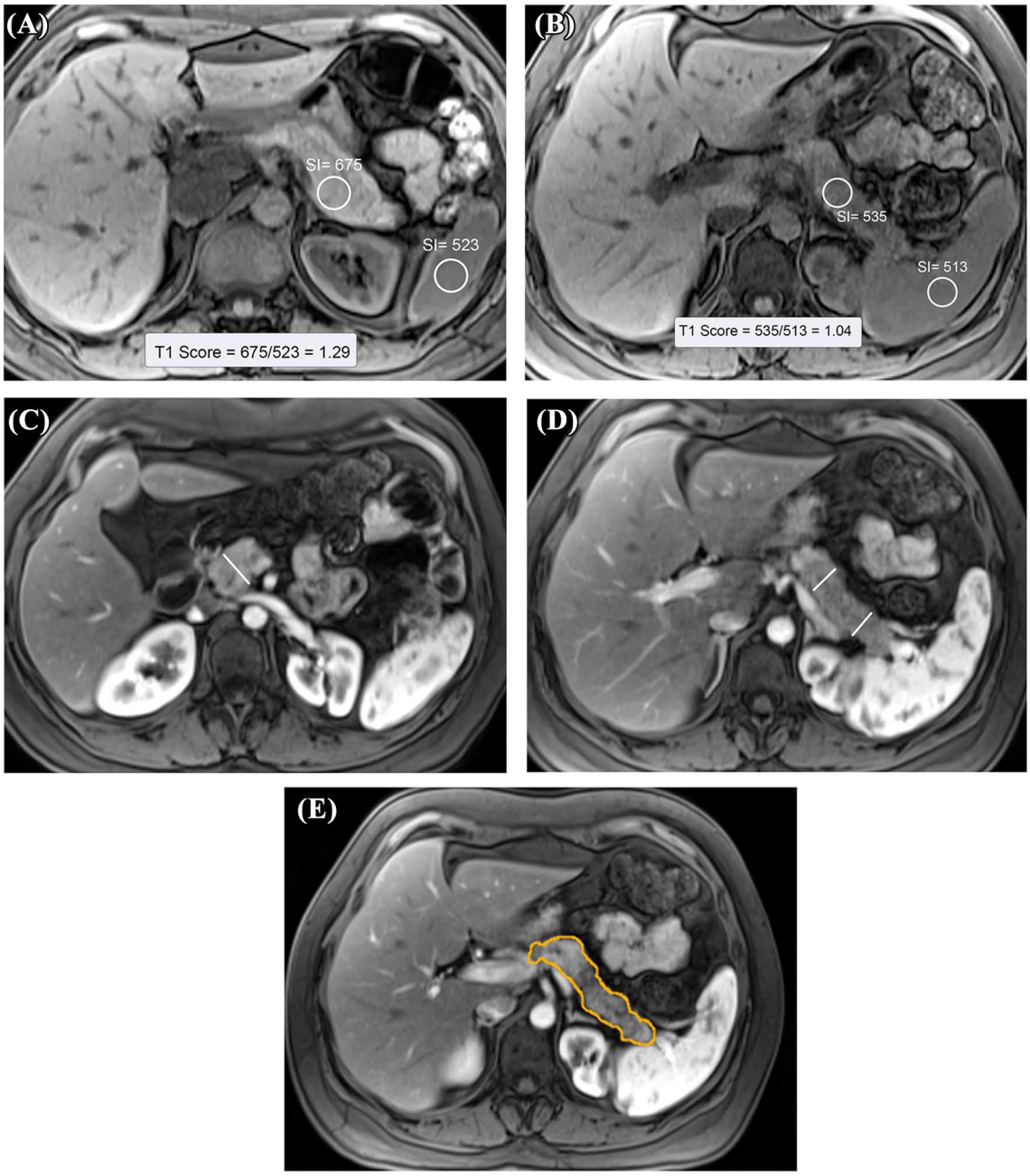

Fig. 2.

Measuring T1 SIR (T1 Score) of the pancreas. **A** 46-year-old female in the control group with no known pancreas disease. Axial, unenhanced, fat-suppressed T1W gradient-echo image shows the region of interest measurements of the pancreatic tail and spleen. The T1-weighted signal intensity of the pancreas is higher than that of the spleen (T1 score: 1.29). **B** 26-year-old female with CP. Axial, unenhanced, fat-suppressed T1W gradient-echo image. T1 signal intensity of the pancreas is significantly lower (T1 Score of 1.04) compared to the control participant in **A**. **C** 38-year-old male with CP. This post-contrast T1W image obtained during the arterial phase shows pancreatic head diameter measurement. Calipers

were placed perpendicular to the pancreatic duct. **D** 38-year-old male with CP. Measurement of pancreatic diameter in the pancreatic body and tail is shown on the post-contrast T1W image obtained during the arterial phase. Calipers were placed perpendicular to the pancreatic duct. **E** 38-year-old male with CP. Measurement of the pancreatic volume shown on contrast-enhanced T1W image with fat suppression. Contours were drawn manually at multiple levels using an independent workstation

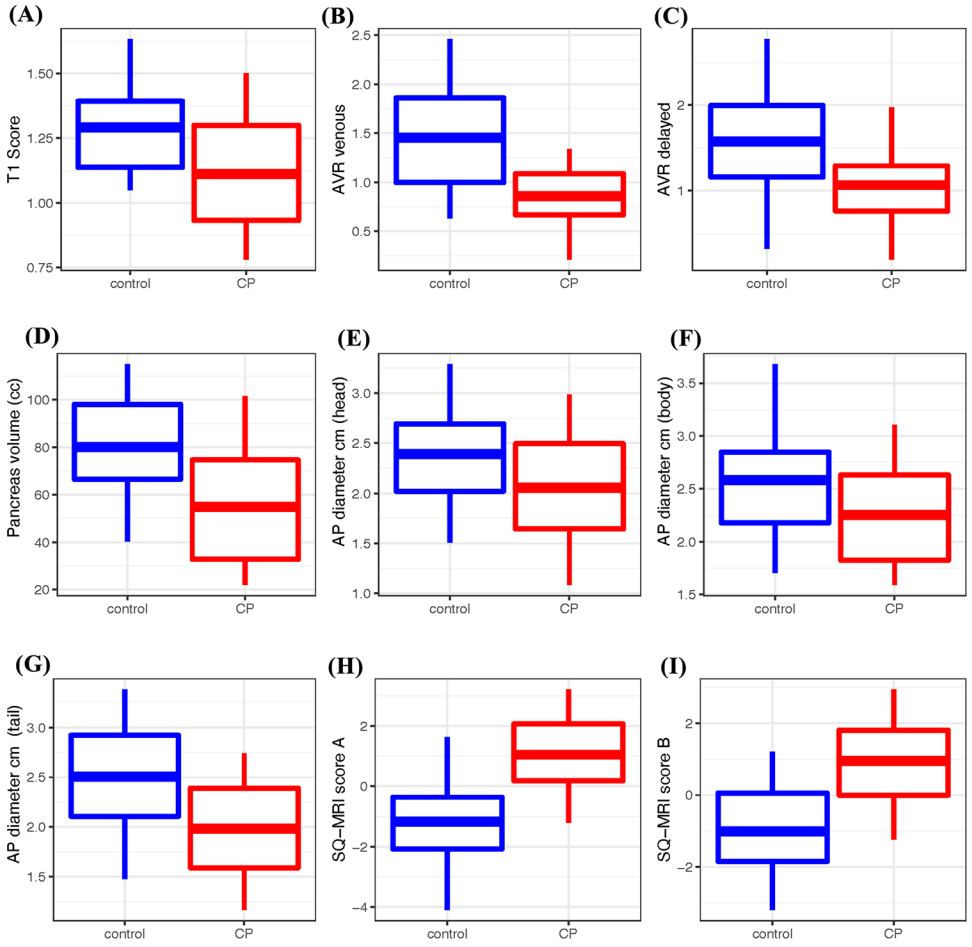

Fig. 3.

Boxplot of the MRI parameters and SQ-MRI scores in control and CP participants. The SQ-MRI scores using Model A and Model B are significantly higher in CP

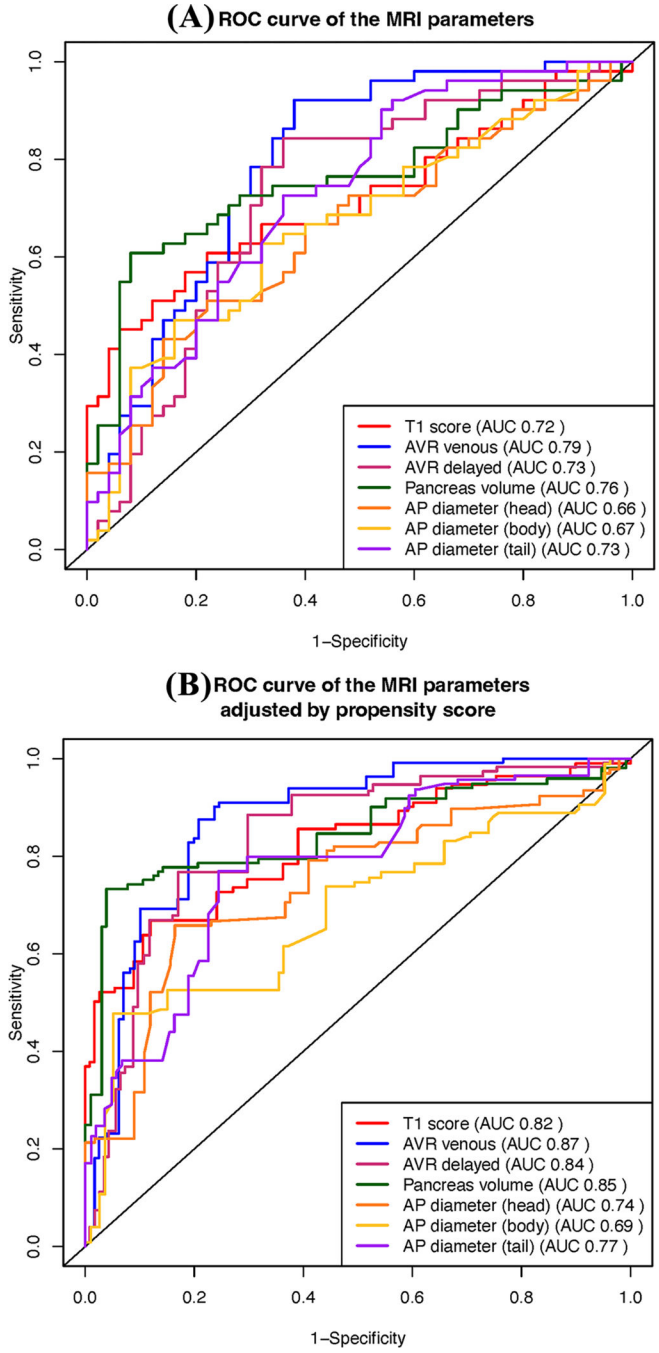

Fig. 4.

Comparison of ROC curves of the seven MRI parameters with (**A**) and without (**B**) propensity score adjustment. The ROC analysis suggests that all seven MRI parameters can be helpful in the evaluation of CP. The propensity score adjustment quantifies the expected difference in MRI parameters between the CP and control groups with similar but not identical demographic characteristics

Table 1

Baseline characteristics of participants in the control and CP groups.

	Control	CP	*p* *
n	50	51	
Age	50.3 (14.0)	53.9 (14.6)	0.20
BMI (kg/m^2)	27.0 (4.9)	26.9 (5.5)	0.79
Male *n* (%)	26 (52.0)	21 (41.2)	0.32
Race *n* (%)			
White	38 (82.6)[4]	45 (91.8)[2]	0.38
Black	5 (10.9)	2 (4.1)	
Asian	3 (6.5)	2 (4.1)	
Smoking *n* (%)			
Never	29 (61.7)[3]	27 (54.0)[1]	0.72
Past	12 (25.5)	14 (28.0)	
Current	6 (12.8)	9 (18.0)	
Drinking status *n* (%)			
Never	5 (10.6)[3]	12 (24.0)[1]	<0.001
Past	6 (12.8)	24 (48.0)	
Current	36 (76.6)	14 (28.0)	
Alcohol intake *n* (%)			
Abstainer	5 (12.2)[9]	12 (25.0)[3]	0.57
Light	6 (14.6)	8 (16.7)	
Moderate	12 (29.3)	10 (20.8)	
Heavy	13 (31.7)	14 (29.2)	
Very heavy	5 (12.2)	4 (8.3)	
Alcohol etiology of CP *n* (%)			
Yes	NA	8 (16.0)[1]	N/A
Diabetes mellitus present *n* (%)			
Yes	NA	14 (28.0)[1]	N/A
Calcification $^{\Psi}$ *n* (%)			
Yes	NA	26 (52.0)[1]	N/A
Exocrine pancreatic dysfunction (EPD) present *n* (%)			
No	NA	23 (76.7)	N/A
Yes		7 (23.3)	
Not tested†		21	

Mean (standard deviation) is reported for age and BMI. Count (column percentage) is reported for categorical variables. Superscript numbers indicate the counts of missing values, which are excluded from the percentage calculation

* Wilcoxon test for continuous variables and Fisher exact test for categorical variables were used

$^{\Psi}$ Calcifications were assessed on CT

[†]Participants in the “EPD not tested” group include those with no known EPD at enrollment who did not undergo a per-protocol assessment with fecal elastase testing

Table 2

Univariate comparison of each MRI parameter between controls and CP participants. CP participants had a significantly lower mean T1 Score, AVR venous, AVR delayed, volume, and diameter in the head, body, and tail

	Control	CP		
	Mean (SD, Q25, Q50, Q75)	Mean (SD, Q25, Q50, Q75)	*p*-value	AUC
T1 Score	1.29 (0.21, 1.14, 1.25, 1.39)	1.11 (0.26, 0.93, 1.08, 1.30)	0.0002	0.72
AVR venous	1.45 (0.72, 1.00, 1.31, 1.86)	0.86 (0.37, 0.67, 0.88, 1.09)	<0.0001	0.79
AVR delayed	1.57 (0.73, 1.16, 1.55, 1.99)	1.07 (0.55, 0.76, 1.04, 1.29)	0.0002	0.73
Pancreas volume	80.00 (22.77, 66.46, 78.28, 98.13)	54.97 (28.24, 32.73, 47.70, 74.60)	<0.0001	0.76
Diameter (head)	2.39 (0.54, 2.02, 2.44, 2.69)	2.05 (0.60, 1.65, 1.94, 2.50)	0.0039	0.66
Diameter (body)	2.58 (0.55, 2.18, 2.59, 2.85)	2.25 (0.51, 1.83, 2.23, 2.63)	0.0023	0.67
Diameter (tail)	2.51 (0.66, 2.11, 2.44, 2.92)	1.98 (0.54, 1.59, 2.04, 2.39)	<0.0001	0.73
SQ-MRI score A	−1.17 (1.78, −2.07, −1.04, −0.36)	1.05 (1.33, 0.19, 0.97, 2.07)	<0.0001	0.82
SQ-MRI score B	−1.01 (1.48, −1.84, −0.91, 0.05)	0.95 (1.34, −0.002, 1.11, 1.80)	<0.0001	0.81

Data reported as mean (standard deviation, 25th quantile, median, 75th quantile). The *p*-value is calculated from a two-sample *t*-test. AUCs for SQ-MRI scores are calculated using 200 internal cross-validations

Abdom Radiol (NY). Author manuscript; available in PMC 2023 November 15.

Table 3

Linear regression analysis evaluating associations of MRI parameters with demographic and disease-related risk factors in CP participants.

	T1 Score		AVR venous		AVR delayed		Volume		Diameter (head)		Diameter (body)		Diameter (tail)	
	Est	***p***	**Est**	***p***	**Est**	***p***	**Est**	***p***	**Est**	***p***	**Est**	***p***	**Est**	***p***
Intercept	0.69	0.084	0.06	0.911	−0.25	0.737	20.63	0.570	0.66	0.400	1.95	0.009	2.16	0.003
Age (years)	0.01	0.113	0.0002	0.966	0.001	0.902	−0.02	0.952	0.004	0.585	−0.01	0.432	−0.003	0.670
Male	−0.06	0.602	−0.09	0.565	−0.13	0.546	−3.10	0.760	0.19	0.396	0.04	0.822	0.24	0.224
Race [†]														
White	0.19	0.449	0.65	0.069	0.73	0.131	39.40	0.095	0.86	0.094	−0.26	0.560	0.18	0.671
Black	0.25	0.459	0.74	0.125	0.65	0.318	54.88	0.090	1.34	0.057	−0.18	0.773	0.46	0.442
BMI (kg/m^2)	0.001	0.934	0.004	0.810	0.03	0.136	0.41	0.674	0.03	0.139	0.03	0.112	−0.01	0.523
Smoking [†]														
Current smoker	−0.04	0.778	−0.19	0.363	−0.31	0.270	−16.11	0.247	−0.32	0.282	0.22	0.413	0.01	0.960
Past smoker	−0.08	0.555	−0.02	0.933	−0.23	0.360	4.55	0.711	−0.32	0.236	0.03	0.893	0.55	0.024 *
Drinking status [†]														
Past	0.05	0.854	0.16	0.657	0.14	0.785	6.07	0.806	−0.40	0.451	0.91	0.067	0.11	0.810
Current	0.02	0.958	0.17	0.664	0.002	0.998	2.75	0.918	−0.59	0.315	0.66	0.215	−0.03	0.955
Drinking category [†]														
Light	−0.11	0.672	0.19	0.614	0.07	0.886	−35.25	0.162	−0.33	0.540	−1.02	0.042 *	−0.04	0.927
Moderate	0.03	0.905	0.06	0.879	0.14	0.776	−5.40	0.826	0.45	0.401	−0.83	0.093	−0.31	0.498
Heavy	−0.01	0.960	−0.29	0.456	−0.24	0.657	−34.48	0.189	0.07	0.902	−1.04	0.047 *	−0.57	0.247
Very heavy	−0.25	0.384	−0.11	0.794	−0.12	0.825	−38.53	0.162	−0.17	0.778	−1.25	0.024 *	−0.87	0.095
Diabetes present	0.02	0.872	0.10	0.561	−0.11	0.628	10.50	0.361	−0.42	0.100	−0.14	0.543	0.08	0.723
Calcifications [¥]														
Present	0.06	0.632	−0.02	0.891	−0.14	0.560	7.31	0.521	0.14	0.567	0.41	0.070	0.30	0.170
EPD status [†]														
EPD present	−0.15	0.303	0.05	0.804	0.28	0.329	−14.63	0.295	−0.24	0.426	−0.57	0.041 *	−0.18	0.482
EPD not tested	−0.10	0.410	0.05	0.784	−0.17	0.479	−3.96	0.728	−0.19	0.445	−0.29	0.199	−0.21	0.340

This table shows the estimated regression coefficients and *p*-values of the covariates from the linear model associating patient characteristics to individual MRI parameters.

The estimated regression coefficient quantifies the mean change in the MRI parameter associated with a unit change in covariate

AVR arterial-to-venous ratio, *BMI* body mass index, *EPD* exocrine pancreatic dysfunction, *p p*-value

* Statistically significant at a critical value of 0.05

Ψ Calcifications were assessed on CT

† Reference categories: others in race, never smokers in smoking, never drinker in drinking status, abstainer in drinking category, and EPD status no